Chemical Engineering Science 248 (2022) 117176

Contents lists available at ScienceDirect

Chemical Engineering Science

journal homepage: www.elsevier.com/locate/ces

Choked liquid flow in nozzles: Crossover from heterogeneous to homogeneous cavitation and insensitivity to depressurization rate

Øivind Wilhelmsen [a,b,*], Ailo Aasen [a]

[a] SINTEF Energy Research, Sem Sælands vei 11, NO-7034 Trondheim, Norway
[b] NTNU, Department of Chemistry, Høgskoleringen 5, NO-7491 Trondheim, Norway

HIGHLIGHTS

- We present new delayed equilibrium models to describe the two phase transition.
- The new models are used to describe the critical mass flow rate in nozzles.
- For CO_2, the models deviate 11% from data with no fitting parameters.
- For water, the agreement with experiments is 3%.
- A crossover from homogeneous to heterogeneous nucleation is found.

ARTICLE INFO

Article history:
Received 17 June 2021
Received in revised form 1 October 2021
Accepted 3 October 2021
Available online 8 October 2021

Keywords:
Critical mass flow
Metastability
Phase transition models
Nozzle
Constrained flow
Ejectors
CO_2
H_2O

ABSTRACT

The critical mass flow rate is the maximum flow rate that can pass through a constrained geometry such as a nozzle. For liquid CO_2, it has been shown that homogeneous relaxation models systematically underpredict the critical mass flow rate. In this work, we demonstrate that a delay of the phase transition is necessary to reproduce experiments. To analyze this in further detail, two methodologies are presented: (1) the delayed homogeneous relaxation model (Delayed HRM), and (2) the metastable isentrope model (MIM). Delayed HRM is a relaxation model that can readily be incorporated into a spatially distributed description of the fluid flow, e.g. in ejectors. MIM assumes isentropic flow and instantaneous equilibrium up to the limit of metastability, and yields a geometry-independent critical mass flux as the solution of a set of algebraic equations. We compare the two methodologies to available experimental data on the critical mass flow rates of CO_2 and H_2O through nozzles, finding that they give nearly identical predictions. This suggests that the critical mass flow rate is mostly determined by the achievable degree of metastability before onset of phase change, and is rather insensitive to dynamic variables such as the depressurization rate or the rate of relaxation towards equilibrium. Using the limit of metastability predicted by homogeneous nucleation theory works well at high temperatures, rendering the methodologies completely predictive. They deviate on average 11% from experimental data on CO_2, and thus outperform homogeneous relaxation models by a large margin, even when the latter employs several fitted parameters. Especially good agreement was found with experiments that employ a lubrication oil, which is hypothesized to suppress heterogeneous nucleation. The limit of superheat at lower temperatures must be described by heterogeneous nucleation theory. For water and CO_2 we find a crossover between homogeneous and heterogeneous nucleation at $T \approx 590$ K and $T \approx 285$ K respectively. Moreover, the predicted limit of superheat falls on a single curve in the temperature–pressure space of water, and we present an empirical correlation of this curve. By combining this expression with the above methodologies, we obtained an average deviation of 3% with available experimental data on H_2O mass flow rates.
© 2021 The Authors. Published by Elsevier Ltd. This is an open access article under the CC BY license (http://creativecommons.org/licenses/by/4.0/).

1. Introduction

When a liquid flows through a nozzle, the flow rate tends to increase as the nozzle outlet pressure is lowered. This only holds up to a point; below a certain outlet pressure the flow rate remains constant at a maximal value (Amos and Schrock, 1983). This is

* Corresponding author at: NTNU, Department of Chemistry, Høgskoleringen 5, NO-7034 Trondheim, Norway.
E-mail address: oivind.wilhelmsen@ntnu.no (Ø. Wilhelmsen).

https://doi.org/10.1016/j.ces.2021.117176
0009-2509/© 2021 The Authors. Published by Elsevier Ltd.
This is an open access article under the CC BY license (http://creativecommons.org/licenses/by/4.0/).

referred to as critical flow or, alternatively, choked flow. Modeling of critical flow in constrained geometries has several engineering applications, including loss-of-coolant accidents in nuclear reactors (Xu et al., 1997), CO_2 transport and storage (Zhou et al., 2014; Fan et al., 2018), space travels (Simoneau and Hendricks, 1979), as mixing devices (Zhu et al., 2018), and cooling of semiconductors (Kim and Mudawar, 2015). In accidents where a pressurized fluid starts leaking, the critical mass flow rate is a crucial input to the risk assessment; unfortunately, with conventional models the leakage rate can be significantly underpredicted (Boccardi et al., 2005).

Another application is the modeling of ejectors (also called jet pumps), which are frequently used in refrigeration cycles for expansion work recovery (Ringstad et al., 2020). In ejectors, the high-pressure stream is sent through a nozzle to accelerate it and decrease its pressure, which then sucks in a low-pressure stream, entrains it, and increases its pressure. Since the flow of this high-pressure motive stream is critical for efficient ejectors, predicting the critical flow rate correctly is crucial for accurately modeling the ejector efficiency (Ringstad et al., 2020).

Due to the widespread use of CO_2 as refrigerant, much work has been devoted to modeling the critical mass flow of CO_2 through motive nozzles in ejectors (Nakagawa et al., 2009; Angielczyk et al., 2010; Banasiak and Hafner, 2011; Banasiak and Hafner, 2013; Palacz et al., 2017; Haida et al., 2018; Giacomelli et al., 2019; Angielczyk et al., 2019; Bodys et al., 2020), as recently reviewed in detail by Ringstad et al. (2020). The motive stream can undergo a phase transition in the nozzle, and modeling this phase transition is key to predicting the critical mass flow. Many strategies for the modeling of this phenomenon exist, but in recent decades, the most popular approach has been to adopt coarse-grained relaxation models (Downar-Zapolski et al., 1996; Attou and Seynhaeve, 1999; Banasiak and Hafner, 2011; Banasiak and Hafner, 2013; Palacz et al., 2017; Bodys et al., 2020). A key feature of such models is that a fraction of the incipient phase develops instantaneously upon crossing the phase coexistence curve. Much of the effort in the literature has thus been to regress empirical relaxation models that aim to describe the rate of transition to a two-phase equilibrium (Downar-Zapolski et al., 1996; Attou and Seynhaeve, 1999; Banasiak and Hafner, 2011; Banasiak and Hafner, 2013; Palacz et al., 2017; Bodys et al., 2020).

Unfortunately, these models require several empirical fitting parameters, and have limited accuracy outside of the domain where they have been regressed. This is illustrated well by the recent work by Bodys et al. (2020), where a two-dimensional computational fluid dynamics model was employed; five fitted parameters were used in the relaxation model. Moreover, as shown by Ringstad et al. (2020), the empirical models systematically *underpredict* the critical mass flow rate, although less so than the homogeneous equilibrium model where it is assumed that the fluid is at thermodynamic equilibrium at all times (Ringstad et al., 2020). This strongly suggests that part of the governing physics is missing from the description. Part of the purpose of this work is to emphasize that what is missing from calculations of critical mass flow rates with CO_2 is to properly account for the metastable, single-phase fluid regime prior to the emergence of a new phase.

It is common knowledge that pure water must be cooled well below the coexistence temperature of 273 K before ice forms, in particular in small geometries with smooth surfaces (Wahl et al., 2020). The onset of ice formation is known as the limit of supercooling, and is perhaps the best known example of a limit of metastability, or "nucleation limit". Similarly, the experimentally attainable limit where a superheated liquid spontaneously transforms into vapor is known as the *limit of superheat* (Blander and Katz, 1975; Debenedetti, 1996). The most popular experimental technique for measuring the limit of superheat is the droplet explosion method, a technique dating back to the early work of Wakeshima and Takata (1958) and Moore (1959). The droplet explosion method remains the most popular technique to date (Eckhoff, 2014; Avedisian, 1985), and represents one of the techniques that can bring the liquid closest to the spinodal limit, which is the intrinsic limit of stability of a homogeneous fluid (Lienhard and Karimi, 1981; Lienhard et al., 1986). In a previous work, we showed that homogeneous nucleation theory can accurately predict the experimentally determined limit of superheat, both for pure components and mixtures (Aursand et al., 2017).

A delayed onset of the two-phase transition in fluid flow has been discussed in the literature, albeit not for CO_2, see e.g. (Liao and Lucas, 2017) for a recent review. In Fig. 13 of Ref. (Liao and Lucas, 2017), Liao and Lucas give an excellent overview of what is referred to as "Boiling delay models". Alamgir et al. (1980), Alamgir and Lienhard (1981) pioneered this modeling approach, forming the basis for subsequent more accurate modifications such as that by Yin et al. (2020). In these models, the depressurization rate enters as a key variable. Levy and Abdollahian argued that the dependence on depressurization rate increases the complexity of the calculations (Levy and Abdollahian, 1982). Deligiannis and Cleaver (1992) attempted to evaluate this hypothesis by correlating the pressure drop to the depressurization rate. They found a rather poor match, but suggested that the deviations could be explained by inconsistencies in the experimental measurements.

In this work, we shall investigate this hypothesis further by incorporating the nucleation limit into a description of fluid flow through constrained geometries by formulating a new "Delayed Homogeneous Relaxation Model". This model can readily be incorporated into computational fluid dynamics (CFD) simulations or as part of mathematical models of ejectors or nozzles for a more precise representation of the critical mass flow rate. We will also discuss the "Metastable Isentrope Model", where the critical mass flow rate is obtained by solving a set of algebraic equations without any need for elaborate CFD simulations. By comparing to experimental data on CO_2 and H_2O, we will show that the nucleation limit plays a crucial role in predicting critical mass flow rates. This is an important message to the community working on CO_2-ejectors, as only homogeneous relaxation models have been considered thus far (Ringstad et al., 2020). Furthermore, we shall demonstrate that the experimental critical mass flow rates can be reproduced to a high accuracy without using the depressurization rate as a variable. Our most important finding however, is that in the high temperature regime, the limit of metastability achieved in nozzles is adequately represented by homogeneous nucleation theory with a crossover to heterogeneous nucleation theory occurring at lower temperatures. Thus, at high temperatures, the presented framework becomes *completely predictive*, with large gains in accuracy over existing approaches that use several fitting parameters.

2. Theory

In Section 2.1 we present the governing equations for fluid flow, and introduce two closure relations for the thermodynamics: the Homogeneous Equilibrium Model (Section 2.1.1) and the Delayed Homogeneous Relaxation Model (Section 2.1.2). Section 2.2 discusses a simplified, isentropic version of these flow models that can be solved algebraically. Finally, Section 2.3 touches on some numerical issues and Section 2.4 describes how the nucleation limits were calculated.

2.1. Full flow model

We consider a converging nozzle geometry as the one depicted in Fig. 1, which can be characterized by the inlet diameter d_i, the

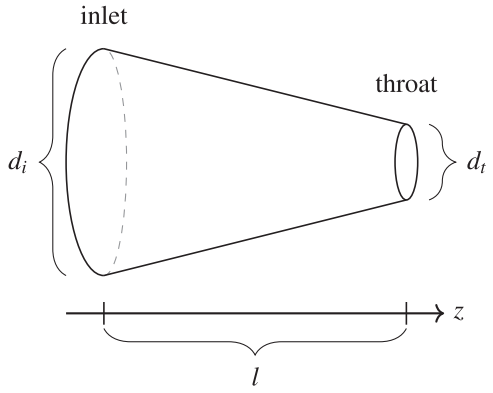

Fig. 1. Illustration of a converging nozzle geometry.

throat diameter d_t, and the horizontal length l. A fluid enters at $z = 0$, and for specified inlet conditions of the fluid and nozzle geometry, it is of interest to determine the maximum possible mass flow rate. We shall consider a steady-state, area-averaged plug-flow model with no heat flow from the walls. The value of the total mass flow, $\dot{m}_{\text{tot}}$, is constant, as expressed by the continuity equation

$$\frac{\partial(A\rho v)}{\partial z} = \frac{\partial \dot{m}_{\text{tot}}}{\partial z} = 0, \tag{1}$$

where A is the area, ρ is the area-averaged density, v is the velocity in the flow direction and z is the spatial coordinate in the flow direction. The momentum equation is

$$\frac{\partial(A(\rho v^2 + P))}{\partial z} = P\frac{\partial A}{\partial z} - \frac{\tau_p f \rho v^2}{8}, \tag{2}$$

where f is the Fanning friction factor, P is the pressure and τ_p is the local perimeter. The two-phase viscosity was approximated by Effective medium theory, which was originally derived for the averaged thermal conductivity and successfully tested by Awad and Muzychka (2008) for the average viscosity of vapor–liquid mixtures of various refrigerants. The friction factor f was estimated by the empirical correlation by Churchill, where the wall roughness was assumed to be 1 μm (Churchill, 1977). The energy balance is

$$\frac{\partial\left(A\rho v(h + \frac{v^2}{2})\right)}{\partial z} = 0 \Rightarrow \frac{\partial\left(h + \frac{v^2}{2}\right)}{\partial z} = 0, \tag{3}$$

where h is the mass-specific enthalpy of the mixture. We have here neglected a possible heat flux from the walls to the fluid, which is expected to be a good assumption due to the high mass flow rate through the nozzle. Eqs. 1–3 comprise three equations for the four quantities (v, ρ, P, h), which will be closed with a relation between the thermodynamic properties (ρ, P, h). This work will consider two closures: the homogeneous equilibrium model, and a nonequilibrium relaxation model.

2.1.1. The homogeneous equilibrium model

In the homogeneous equilibrium (HEM) model, the closure is accomplished by assuming thermodynamic equilibrium at all states along the flow path. This entails solving one algebraic equation at every spatial step in the integration of the ordinary differential equations. With an initial guess for the velocity one can compute h and p by use of Eqs. (2) and (3). An enthalpy–pressure flash calculation is then used to identify the temperature, vapor fraction and compositions in each phase. By using an equation of state (EoS), the density ρ_{EoS} is thus computed. Furthermore, ρ is next computed from Eq. (1). At every spatial position we require in the HEM model that the following residual is zero

$$\text{res}(v) = \frac{\dot{m}_{\text{tot}}}{Av} - \rho_{\text{EoS}}(h, P). \tag{4}$$

2.1.2. Delayed homogeneous relaxation model

For a metastable liquid, it is possible to increase the critical mass flow rate beyond the value given by the homogenous equilibrium model. We define the degree of metastability as

$$\Delta T(P) = T_{\text{m}}(P) - T_{\text{sat}}(P), \tag{5}$$

where T_{m} is the temperature of the metastable fluid phase and T_{sat} is the temperature of the saturated fluid phase at the same pressure P. The quantity ΔT is positive for evaporation of a metastable liquid and negative for condensation of a metastable vapor, and its maximum (minimum) value is the nucleation limit for evaporation (condensation), ΔT_{lim}.

Aursand et al. (2017) showed that the nucleation limit of a fluid can be accurately predicted by use of homogeneous nucleation theory, also for mixtures. At temperatures close to the critical temperature, we shall employ the same theory as presented by Aursand et al. (2017). At lower temperatures, there is a need to use heterogeneous nucleation theory, since the activation energy to initiate the phase change is lowered by cracks and imperfections at the nozzle structure. Further details on the computation of ΔT_{lim} can be found in Section 2.4.

An input parameter in the determination of ΔT_{lim} is the surface tension. For pure fluids the surface tension is usually tabulated. For mixtures where the surface tension is not tabulated, one can employ e.g. density theory gradient theory with a geometrical mixing rule based on the pure component parameteters (see Refs. Aasen et al., 2018; Wilhelmsen et al., 2014 for further details).

We will focus on the case where a single-phase liquid enters the nozzle. As the liquid flows towards the throat, it may become metastable and ΔT will increase. At some location z_l the metastability of the liquid matches ΔT_{lim}, that is

$$\Delta T(P(z_l)) = \Delta T_{\text{lim}}(P(z_l)). \tag{6}$$

After this location the phase change begins, and the metastable single-phase fluid relaxes towards a two-phase equilibrium. In this work we have used the simple relaxation model

$$\frac{d\Delta T}{dt} = -\frac{\Delta T}{\tau}, \tag{7}$$

where $\tau = 10^{-4}$ s. Eq. (7) can readily be replaced by a more sophisticated relaxation model that includes a dependence with respect to the fluid state, but we shall show in Section 3.3 that the predictions of the critical mass flow rates are very insensitive with respect to the exact choice of τ.

Before the nucleation limit is reached, the thermodynamic properties are computed as those of a pure liquid. After the nucleation limit, in the relaxation regime, the temperatures of the phases are unequal, but the extensive properties of the fluid can still be calculated as a sum of extensive properties of the phases. In either case, the necessary consistency criteria are formulated by requiring that the following residuals are zero:

$$\text{res}_1 = \beta/\rho_{\text{EoS}}^{\text{vap}}(T^{\text{sat}}(P), P) + (1-\beta)/\rho_{\text{EoS}}^{\text{liq}}(T^{\text{sat}}(P) + \Delta T, P) - \frac{Av}{\dot{m}_{\text{tot}}}, \tag{8}$$

$$\text{res}_2 = \beta h_{\text{EoS}}^{\text{vap}}(T^{\text{sat}}(P), P) + (1-\beta)h_{\text{EoS}}^{\text{liq}}(T^{\text{sat}}(P) + \Delta T, P) - h, \tag{9}$$

where β is the mass fraction of vapor, and superscripts vap, liq and sat refer to vapor, liquid and the saturated phase. For metastable liquids, $\beta = 0$ before evaporation begins.

2.2. Metastable isentrope model for evaporating flows

We find that the entropy production in the nozzle prior to phase change is usually small, and so the entropy is, to a good approximation, conserved. Assuming the flow to be isentropic, the flow model can be solved algebraically: Every state on the isentrope corresponds to a unique value of the enthalpy h, and from Eq. (3), every value of the enthalpy corresponds to a unique flow velocity $v = \sqrt{2(h_0 - h)}$, where h_0 is the stagnation enthalpy corresponding to zero velocity. Since the mass flux $\Phi(z) = \dot{m}_{\text{tot}}/A(z)$ is determined by the total mass flow and the geometry, the thermodynamic state and the flow velocity at each position can be found by solving

$$\Phi(z) = \rho\sqrt{2(h_0 - h)}. \tag{10}$$

The right-hand side of Eq. (10) has a maximum value along a given isentrope, which in this model corresponds to the critical mass flux for the isentropic flow. For a single-phase liquid, the right-hand side is a strictly decreasing function of pressure, which implies that the maximum mass flux occurs at the lowest possible pressure of the isentrope that can sustain a liquid phase, i.e. at the limit of superheat.

We shall refer to this method of predicting the critical mass flux as the Metastable Isentrope Model (MIM). From a physical perspective, this model assumes that the fluid remains single-phase until the superheat limit is reached, at which point the flow chokes and critical flow is established. The choke point occurs where Φ_m is largest, namely at the throat of the nozzle. A maximum in the mass flux can also be found if one assumes thermodynamic equilibrium, and the resulting model corresponds to an isentropic version of HEM. For both HEM and MIM, a key feature of the isentropic assumption is that the critical mass flux is only a function of the stagnation state and independent of the nozzle geometry. This contrasts with the delayed boiling model by Alamgir et al. (1980), Alamgir and Lienhard (1981) and subsequent modifications (Liao and Lucas, 2017), where the degree of achieved metastability also depends on the depressurization rate.

Further simplifications are possible in certain regions of the phase diagram. For example, if one assumes that the liquid is incompressible along the isentrope, one can write the following relation for evaporating flows:

$$\Phi_m = \sqrt{2\rho_{\text{liq}}(P_0 - P_{\text{t}})}, \tag{11}$$

where P_0 is the stagnation pressure, P_{t} is the pressure at the throat, and ρ_{liq} is the liquid mass density. In this case, isentropes are especially simple to characterize: straight lines in the temperature–pressure space, with a positive slope given by the Gibbs–Duhem relation, $\mathrm{d}P = (\rho_{\text{liq}} s)\mathrm{d}T$, where s is the mass-specific entropy. The slope generally increases at low temperatures, so that isentropes are approximately equal to isotherms.

Assuming that the thermodynamic properties of stable and metastable states are available by use of an accurate equation of state, the crucial step in applying the MIM is to accurately determine the limit of superheat, which in the general case corresponds to the homogeneous or heterogeneous nucleation limit.

2.3. Numerics

All thermodynamic calculations in this work were performed using the most accurate equations of state available, so called multiparameter equations of state. These were interfaced by the in-house, open-source thermodynamic library, Thermopack, which contains a wide selection of EoS and routines for robust phase equilibrium calculations (Wilhelmsen et al., 2017; Aasen et al., 2017; Wilhelmsen et al., 2013).

For calculations in the metastable regions, these EoS are associated with numerical difficulties due to their multiple Maxwell loops which is an hitherto unsolved problem of multiparameter EoS (Wilhelmsen et al., 2017). Using a simpler equation of state, like the Peng–Robinson EoS, is numerically more robust and also computationally faster. Such cubic EoS are, however, known to misrepresent thermodynamic properties such as liquid densities and speeds of sound – properties that are crucial for predicting the critical mass flow rate.

Other relaxation approaches also use metastable phase properties with multiparameter EoS, but these metastable properties are computed by linear extrapolation from the saturation state (Angielczyk et al., 2010; Banasiak and Hafner, 2011). However, to ensure thermodynamic consistency one should rather extrapolate a thermodynamic potential as a function of its canonical variables, such as the Helmholtz energy as a function of (T, V, n), or the Gibbs energy as a function of (T, P, n), where n is the number of particles. To avoid potential consistency issues, we obtained metastable properties directly from the EoS. This was done by first locating the spinodal (Aursand et al., 2017), and then using a bracketing solver between the saturation state and the spinodal state.

Due to the simplicity of the algebraic solution of the isentrope models, the computational cost is negligible compared to the full flow models, and the computational robustness is much better.

2.4. Calculation of metastability limits for nucleation

The mechanism by which condensation and evaporation occur is known as nucleation. Nucleation is an activated process where a free energy barrier must be overcome by thermal fluctuations. A nucleation event is when a cluster of the stable phase (permanently) exceeds a critical size, beyond which further growth is spontaneous. The free energy barrier corresponds the work of formation for the critical cluster. In classical nucleation theory (CNT), the nucleation rate J is given by an Arrhenius rate law,

$$J = K\exp\left(-\frac{W}{k_{\text{B}}T}\right), \tag{12}$$

where W is the work of formation of the critical cluster, k_{B} is Boltzmann's constant, and K is a kinetic prefactor capturing the rate at which thermal fluctuations happen.

2.4.1. Homogeneous nucleation

For homogeneous nucleation, CNT assumes that the critical cluster is spherical, and the nucleation barrier is given by

$$W = \frac{4\pi\sigma R^2}{3}, \tag{13}$$

where R is the radius of the critical cluster and σ is the surface tension. Eqs. 12,13 apply to both condensation and evaporation, although the expressions for K and R differ. Assuming incompressible liquid and ideal gas, one finds

$$R = \frac{2\sigma}{P_{\text{sat}}(T) - P_{\text{liq}}}, \tag{14}$$

for bubble formation in a liquid (Debenedetti, 1996), and

$$R = \frac{2\sigma}{\tilde{\rho}_{\text{liq}} k_{\text{B}} T \ln(P_{\text{vap}}/P_{\text{sat}})}, \tag{15}$$

for droplet formation in a vapor (Debenedetti, 1996). Here $\tilde{\rho}_{\text{liq}}$ is the number density of the liquid phase. The kinetic prefactor for bubble formation in a liquid (Debenedetti, 1996) was calculated as

$$K = \tilde{\rho}_{\text{liq}} \sqrt{\frac{2\sigma}{\pi m}}, \tag{16}$$

where $\tilde{\rho}_{\text{liq}}$ is the number density of the liquid phase and m is the molecular mass. For droplet formation in a vapor, we use (Debenedetti, 1996)

$$K = \frac{P^2}{(k_B T)^2 \tilde{\rho}_{\text{liq}}} \sqrt{\frac{2\sigma}{\pi m}}. \tag{17}$$

The metastability limit for homogeneous nucleation is defined as the state at which the nucleation rate is a few orders of magnitude larger than the timescale of the experiment. For liquids this limit is called the superheat limit, whereas for a vapor it is called the supersaturation limit. For a given pressure, it is obtained by solving for the temperature that yields a given nucleation rate J_{onset}:

$$J(T) = J_{\text{onset}}. \tag{18}$$

We have used $J_{\text{onset}} = 10^{13}$ m^{-3}s^{-1} in this work, but we have performed a sensitivity analysis of this choice in Appendix B. This sensitivity analysis shows that the exact choice of J_{onset} has little influence on the predicted critical mass flow rates.

The thermodynamic properties were computed from the EoS, whereas the surface tensions were computed from the most accurate correlations available (Petrova and Dooley, 2014; Mulero et al., 2012). The above framework can be straightforwardly extended to mixtures, with the caveat that for some mixtures one must add curvature corrections to the surface tension to accurately model the metastability limits (Aasen et al., 2020).

2.4.2. Heterogeneous nucleation

For heterogeneous nucleation, CNT assumes that the critical cluster is a portion of a spherical cluster, and the nucleation barrier is given by

$$W = \frac{4\pi\sigma R^2}{3}\phi, \tag{19}$$

where $\phi \in (0, 1)$ is the heterogeneous work reduction factor. The kinetic prefactor for heterogeneous cavitation was approximated by (Debenedetti, 1996)

$$K = (A/V)\tilde{\rho}_{\text{liq}}^{2/3} \sqrt{\frac{2\sigma}{\pi m}}, \tag{20}$$

where A/V is the surface density. The relevant surface density for this work is given by $4/d_t$, where d_t is the throat diameter. Except for the above modifications, the same procedure as in Section 2.4.1 was used to determine the heterogeneous nucleation limit, with $J_{\text{onset}} = 10^{13}$ m^{-2}s^{-1}.

3. Results and discussion

In the following, we will compare the different methods described in Section 2 to available data on the critical mass flow rate of CO_2 and water in various nozzle geometries. These fluids were chosen due to the extent of available experimental data.

3.1. A closer inspection of the phase diagram of CO_2

We start the discussion with a closer inspection of the phase diagram of CO_2 depicted in Fig. 2. The intrinsic limits of thermodynamic stability, i.e. the spinodals of the vapor and the liquid phases (red dotted lines), lie at higher and lower pressures than the saturation curve (black solid line). The homogeneous nucleation limits for the formation of bubbles and droplets are located between the coexistence curve and the spinodals. Spinodals, nucleation limits and the coexistence curve all merge at the critical point.

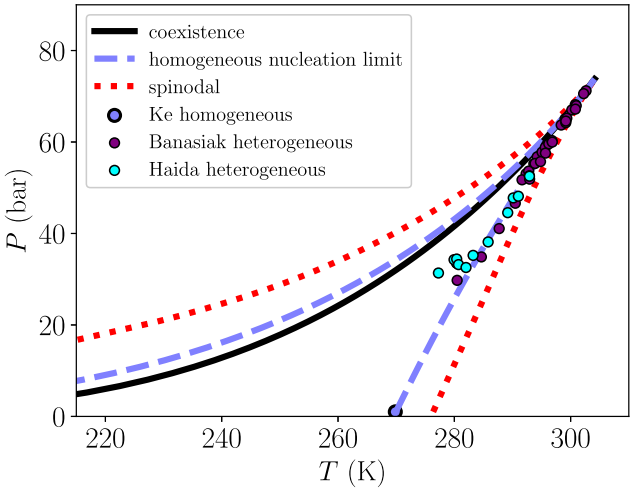

Fig. 2. The coexistence curve calculated by using the Span–Wagner EoS (Span and Wagner, 1996), limits of metastability as predicted from homogeneous nucleation theory, and spinodal limits, plotted using the Span–Wagner equation of state (Span and Wagner, 1996) for carbon dioxide. The experimental estimate of homogeneous limit of superheat is deduced from the work of Ke (2009). The heterogeneous limits of superheat were inferred from the critical mass flux data given by Banasiak and Hafner (2013) and Haida et al. (2018), as discussed in the main text.

In the experiments of Ke (2009), it was found that the highest attainable temperature for liquid CO_2 at 1 bar was 269.85 K. This should therefore be considered a lower bound for the superheat limit at 1 bar. The value by Ke compares favorably with our estimate made with homogeneous nucleation theory: 269.97 K. Since the superheat limit shown in Fig. 2 appears to be predicted very well at the two extremes – the critical pressure and atmospheric pressure – we have confidence in the accuracy of the predictions also at intermediate pressures. This extends the conclusions from previous work (Aursand et al., 2017) to CO_2, i.e. that the limit of superheat of a liquid is accurately predicted by classical homogeneous nucleation theory.

A closer inspection of the figure reveals that the nucleation limit computed for the vapor phase (pressures higher than the coexistence pressure), lies much closer to the coexistence curve relative to the spinodal, than the corresponding limit for the liquid phase. This indicates that metastability effects are less important for condensing flows, although vapor isentropes have smaller slopes than liquid isentropes. The attainable degree of liquid superheat along an isobar is seen to increase strongly as the pressure decreases.

3.2. A comparison to established methods for CO_2

To gauge the accuracy of the methods presented in Section 2, their predictions have been compared to experimental data on the critical mass flow rates of CO_2 for operating conditions 9–22 in Ref. (Haida et al., 2018). The homogeneous equilibrium model (HEM) underpredicts the experimental data, on average, by 26.3%. This is as expected, and has motivated the development of several relaxation models that aim to describe the nonequilibrium path to equilibrium between liquid and vapor. A common denominator for all of the established relaxation models presented in Table 1, by Angielczyk et al. (2010), Downar-Zapolski et al. (1996) and modified HRM by Haida et al. (2018) is that they give predictions that fall significantly *below* the experimental data. A strong bias towards underprediction suggests that the models are missing some of the underlying physics. This is further supported by a closer inspection of the previous state-of-the-art Modified HRM by Haida et al. (2018); with three fitting parameters that also

Table 1
Mean absolute percentage deviations (MAPE) and biases have been computed for the operating conditions 9–22 of Ref. Haida et al. (2018) for our models (MIM and Delayed HRM), Also included are the MAPEs for the relaxation models reported by Haida et al. (2018) for the same set of operating conditions.

Model	MAPE	Bias
HEM	26.3%	−26.3%
Angielczyk et al. (2010)	23.6%	−23.6%
Downar-Zapolski et al. (1996)	20.4%	−20.4%
Modified HRM (Haida et al., 2018)	17.8%	−17.8%
Delayed HRM (this work)	11.4%	7.7%
MIM (this work)	11.3%	7.8%

depend on the operating conditions, the modified HRM deviates on average −17.8% from experimental data. We argue that the underlying physics that is missing from these relaxation models is the delayed onset of the phase transition. Both of the methods presented in this work, Delayed HRM and MIM, perform better than previous approaches, having an average deviation of 11.4% and 11.3% without using any fitting parameters. Here, homogeneous nucleation theory has been used to determine the limit of metastability.

3.3. The role of relaxation in determining the critical mass flow

From Table 1, we observe that the performance of Delayed HRM is nearly identical to that of MIM. A closer inspection of each experiment (B) confirms that these two models indeed give nearly identical predictions of the critical mass flow rates for all the cases examined in this work, both for CO_2 and H_2O. Whereas Delayed HRM accounts for the relaxation towards equilibrium, MIM does not, as it only considers the onset of the phase transition. This finding is supported by a parameter study of the relaxation parameter, τ, in Eq. (7). At least for CO_2 and H_2O, we have found that the exact value of τ has a small/negligible influence on the predicted critical mass flow rates in the delayed relaxation model presented in Section 2.1. In fact, upon changing the value of τ from 10^{-2} s to 10^{-6} s we found that the critical mass flow rate never changed by more than 0.01%, although it did affect the evolution of the flow in the diverging section of the nozzle. The choice $\tau = 10^{-4}$ s was found to be a good compromise between numerical problems for $\tau \lessapprox 10^{-6}$ s, and an essentially frozen degree of metastability when $\tau \gtrapprox 10^{-2}$ s. The most important physical phenomenon to predict correctly in order to capture the critical mass flow rate in an evaporating fluid flow is thus the onset of the phase transition.

We emphasize that although Delayed HRM and MIM yield very similar predictions of the critical mass flow rates, their intended areas of use are different. While Delayed HRM similar to established relaxation models must be coupled to a spatially distributed description of the fluid flow (like in CFD or ejector models), the purpose of the MIM as presented here is only to predict the critical mass flow rate by using an equation of state and the estimated limit of metastability as key inputs.

3.4. Using homogeneous nucleation theory to predict the onset of the phase transition

We have plotted the corresponding deviations from the methods presented in this work against the inlet temperature for two different sources of experimental data in Figs. 3a and b. While most of the results from MIM/Delayed HRM fall within the uncertainty for $T > 285$ K, the methods overpredict the experimental measurements at lower temperatures. The reason for this is that we have used *homogeneous nucleation theory* to determine the onset of the phase transition. While homogeneous nucleation theory assumes that the phase transition occurs within the bulk of the fluid, cracks and imperfections at the nozzle walls will lower the activation barrier and thus also move the onset of the phase transition closer to the binodal, reducing the magnitude of $|\Delta T_{\text{lim}}|$. We find that homogeneous nucleation theory predicts the limit of metastability well at high temperatures, and that there appears to be a crossover to heterogeneous nucleation at lower temperatures. This is especially visible for the nucleation limits inferred by experiments, represented by filled circles in Fig. 2. We shall discuss the crossover between homogeneous and heterogeneous nucleation in further detail for H_2O in Section 3.5, as there are more experiments available at lower temperatures for this fluid.

At $T < 285$ K, we observe that MIM/Delayed HRM that uses homogeneous nucleation theory to determine ΔT_{lim} matches better with the experimental data presented by Banasiak and Hafner (2013) (see Fig. 3a) than the experiments used by Banasiak et al. (2015), Haida et al. (2018). The measurements used in the work of Haida et al. (2018) were made with an industrial-grade ejector rig, with higher uncertainty and less careful control of lubrication oil than the measurements of Banasiak and Hafner (2013). One possible reason for this discrepancy is that the experiments used by Ref. Banasiak and Hafner (2013) include 0.5%-2% mass polyalkylene glycol (PAG) lubrication oil, whereas the experiments used by Banasiak et al. (2015), Haida et al. (2018) did not carefully control for this impurity. If the oil can significantly change the critical mass flow rate, this could explain the discrepancy. An illuminating illustration in this regard is Fig. 5 in the paper by Dang et al. (2012), which shows that unlike the other oils examined, the PAG oil in a flow of CO_2 forms a thick film at the wall. An oil film at the nozzle wall will suppress heterogeneous nucleation. Immersing the metastable liquid in a host liquid is, in fact, an established experimental technique for ensuring ideally smooth substrates Caupin and Herbert (2006). These findings indicate that proper use of oil and wall coating could possibly suppress heterogeneous nucleation and allow for higher critical mass flow rates through nozzles, which could be beneficial in process equipment such as ejectors (Banasiak and Hafner, 2011).

In 1958, Hesson and Peck (1958) reported critical mass flow rates of CO_2 through nozzles and orifices, and provided strong evidence that a saturated liquid entering the nozzle reaches high metastabilities with no evaporation ahead of the throat. They also demonstrated that the mass flow through an orifice is much lower than for a converging nozzle, even if the smallest cross section (the throat area) is the same. However, Hendricks et al. (1972) questioned the accuracy of the measured critical flow rates, pointing out that the data indicate that the inlet liquid was in fact slightly subcooled. We have not included the data by Hesson and Peck in Fig. 2 and in the subsequent comparison, as the data are highly inconsistent with the more recent work in Refs. (Banasiak and Hafner, 2013; Haida et al., 2018). However, we have verified that also the data by Hesson and Peck (1958) display the same qualitative behavior as newer works (Banasiak et al., 2015; Haida et al., 2018), namely what appears to be a crossover from homogeneous to heterogeneous nucleation with decreasing temperature.

3.5. Water

Water is among the most frequently studied fluids, and large amounts of experimental data for the critical flow rate through nozzles are available. Unlike CO_2, where experiments are mainly available near the critical point, experimental data for water are available along the whole saturation curve.

For the flow of water through nozzles at inlet temperatures below 590 K, we found that it was necessary to employ heterogeneous nucleation theory to estimate ΔT_{lim}. Heterogeneous nucleation theory uses homogeneous nucleation theory as a basis, and

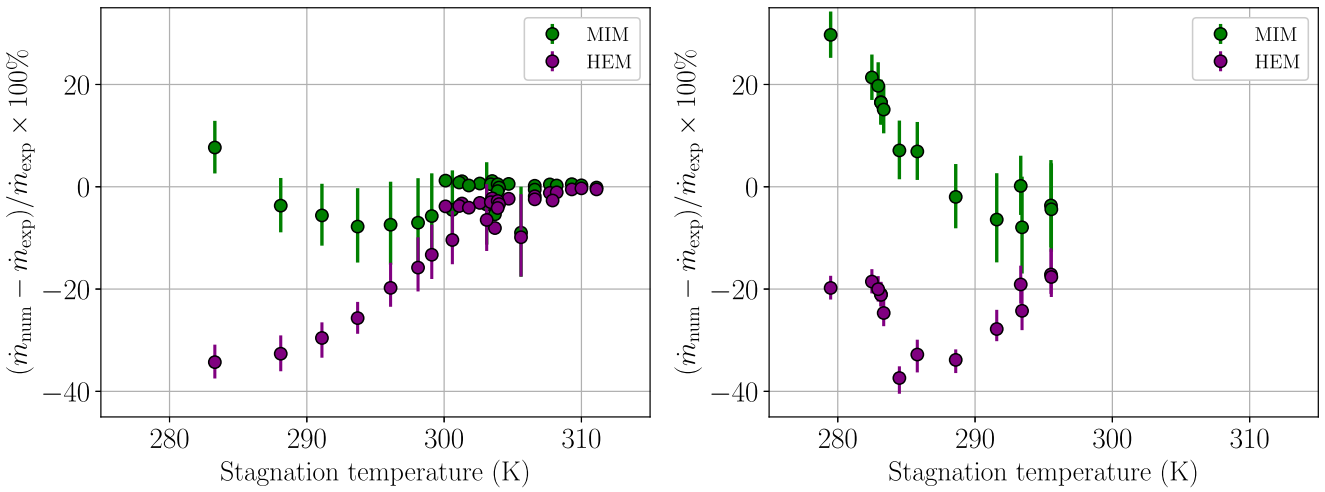

(a) Deviations from Ref. [13]

(b) Deviations from Ref. [15].

Fig. 3. a) Percentage deviation of critical mass flow calculated by HEM and MIM, from the CO_2 measurements by Banasiak and Hafner (2013) for their "N1" geometry. The error bars have been computed by using the experimental uncertainties in the inlet temperature and pressure, in all cases corresponding to evaporating flows. b) Percentage deviation of critical mass flow of HEM and MIM for CO_2, from measurements used by Haida et al. (2018), where the error bars have been computed assuming a temperature uncertainty of ±1 K, and pressure uncertainty ±0.3 bar in the inlet conditions.

employs a work reduction factor that is multiplied with the work of formation (see Section 2.4). This work reduction factor is expected to depend on the temperature dependent contact angle of the fluid with the solid surface and possibly on the nature of the cracks or roughness that initiates the phase transition. The theoretical development of an expression for this work reduction factor represents a very interesting possibility for future work, albeit it falls beyond the scope of the present work. A more practical approach employed in this work is to empirically extract the value for the heterogeneous nucleation limit from experiments.

We started by evaluating the accuracy of the predictions of the homogeneous superheat limit of water by comparing to the experiments by Pavlov and Skripov (1970). As for CO_2, we again find excellent agreement (Fig. 4). To develop an empirical correlation for the temperature of maximum metastability, T_{shl}, we used the critical mass flux measurements of Xu et al. (1997), Burnell (1947) and Friedrich and Vetter (1962). Also for water, we found that MIM and Delayed HRM gave similar results. Using this finding, one can calculate the apparent superheat limit necessary to make the methods match each individual measurement. These apparent superheat limits are plotted in Fig. 4 (black, orange, and purple dots). The experiments were used to regress the empirical expression provided in Appendix A. We emphasize that the various experiments plotted in Fig. 4 span 50 years and come from different research groups that used different experimental facilities and operation conditions, so the collapse onto a single curve is remarkable.

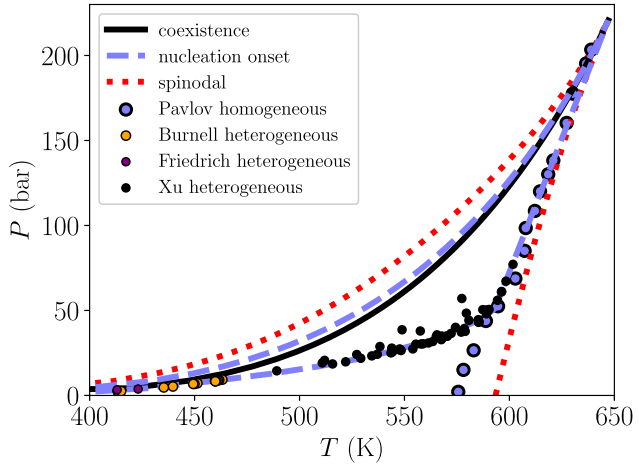

Fig. 4. The coexistence curve, limits of metastability, and spinodal limits for water, plotted using the IAPWS-1995 equation of state (Wagner and Pruß, 2002). Experimental homogeneous nucleation limits are taken from Pavlov and Skripov (1970). The heterogeneous limits of superheat were inferred from the critical mass flux data of Xu et al. (1997), Burnell (1947) and Friedrich and Vetter (1962). The empirical limit of liquid superheat was calculated by the correlation in Appendix A.

That the estimated metastability limits extracted from these experiments collapse onto a single curve strongly suggests that, also for water, the critical mass flow rate is governed by the onset of the phase transition. We are therefore led to conclude that the critical mass flow is independent of the depressurization rate for liquid flows through nozzles, which contradicts the underlying assumptions of the boiling delay models presented by Alamgir et al. (1980), Alamgir and Lienhard (1981) and subsequent modifications (Yin et al., 2020; Liao and Lucas, 2017). As a further verification that the choke point is independent of the depressurization rate, we have in Fig. 5 plotted the deviation in the predicted mass flow of D-HRM against the depressurization rate, which shows that these two variables seem to be uncorrelated. Part of the explanation for this may be that Alamgir and coworkers considered different types of experiments when developing their correlation. Other possible reasons may be that they used a less rigorous nucleation theory or inaccurate thermodynamic data.

Assuming the metastable isentrope model (MIM) to be exact, one can for each critical flow rate measurement calculate a unique value for the temperature where the heterogeneous nucleation limit is reached, T_{lim}. For this value of the superheat limit, one can calculate the value of the heterogeneous work reduction factor that yields $J(T_{\text{lim}}) = J_{\text{onset}}$. Fig. 6 shows the heterogeneous work reduction factors calculated in this way from the water measurements considered in this work. Once again the experiments collapse onto a curve, which is consistent with our hypothesis that the critical mass flow rate can be explained in terms of the nucleation limit. Interestingly the work reduction factor follows an *exponential* dependence on temperature, as also observed by Deligiannis and Cleaver (1992). For simplicity we assumed that

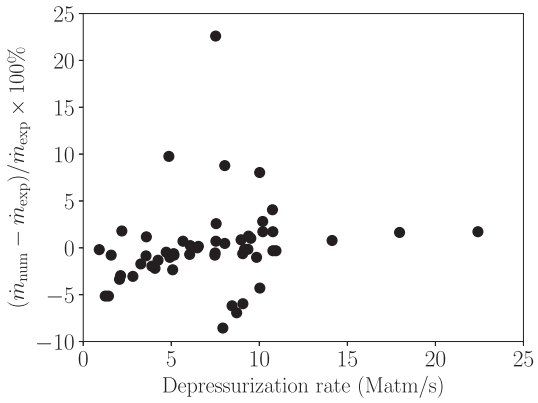

Fig. 5. The error from the metastable isentrope model plotted against the depressurization rate for the critical mass flow measurements for water by Xu et al. (1997) The above results suggest that the variables are uncorrelated.

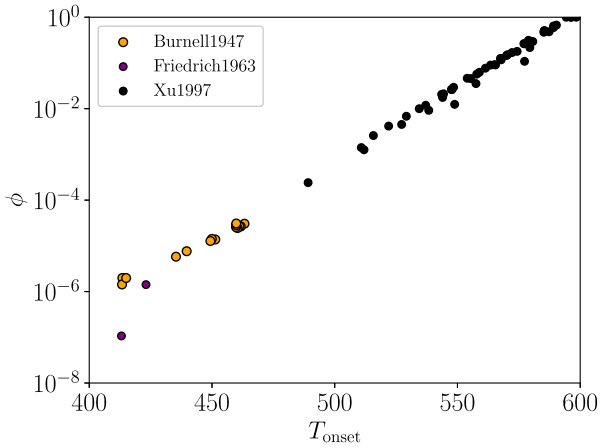

Fig. 6. Heterogeneous work reduction factor for water measurements by Xu et al. (1997), Burnell (1947) and Friedrich and Vetter (1962), plotted against the nucleation onset temperature.

the surface density (A/V) in the kinetic prefactor was the same for all the water measurements, namely that of the nozzle used by Xu et al. (1997).

Plugging the empirical expression for T_{lim} from Appendix A into either MIM or Delayed HRM gives excellent agreement with experimental data for water, with a mean deviation of 3%. In comparison, HEM underpredicts the experimental data by almost 60% on average as shown in Table 2.

Fig. 4 shows what appears to be a crossover from homogeneous nucleation to heterogeneous nucleation, occurring at

$$P_{\mathrm{shl}}^{\mathrm{cross}} \approx 50\mathrm{bar}, \quad T_{\mathrm{shl}}^{\mathrm{cross}} \approx 592.8\mathrm{K}. \tag{21}$$

This crossover corresponds to a maximum penetration into the metastable region, with a pressure difference with respect to the saturation pressure of $P_{\mathrm{sat}} - P_{\mathrm{t}} \approx 60\mathrm{bar}$ at the temperature $T_{\mathrm{shl}}^{\mathrm{cross}}$.

Fig. 7 displays the performance of the methods presented in this work for H_2O, where the largest deviations seen around 440 K are

Table 2
Statistics for the relative deviations in predicted mass flux for MIM and HEM for the water experiments from (Xu et al., 1997; Burnell, 1947; Friedrich and Vetter, 1962)

Model	MAPE	Bias	Max error
MIM	3.0	0.3	20.9
HEM	55.8	−55.8	80.8

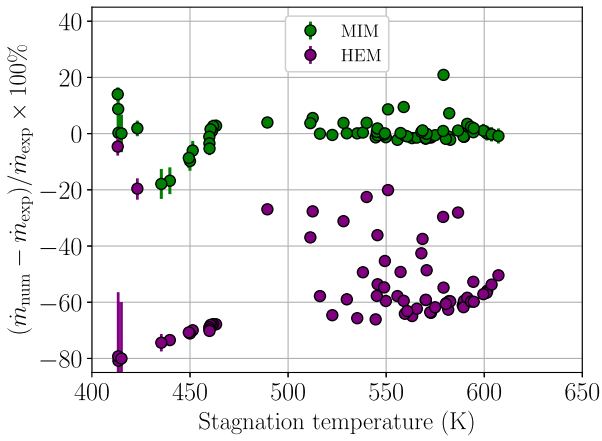

Fig. 7. Percentage deviations of HEM and the metastable isentrope model (MIM) for the water measurements by Xu et al. (1997), Burnell (1947) and Friedrich and Vetter (1962), plotted against the stagnation temperature. The empirical superheat limit was used for the MIM model. The error bars were computed using an uncertainty of ±1 K and ±0.5 bar in the inlet conditions.

with respect to older experimental data with limited accuracy. These coincide with "outliers" in the work reduction factor (cf. Fig. 6), and indicates the need for further validation by new measurements. In summary, an excellent match with experimental data is obtained for water along the whole saturation curve.

4. Conclusion

In this work, we have studied the critical mass flow rate through nozzles, i.e. the maximum possible flow rate for a given inlet state. For liquids, the critical mass flow rate is often determined by the emergence of a second phase. Assuming homogeneous equilibrium in this phase transition leads to underprediction of the critical mass flow rate. The literature on this topic for CO_2 has addressed this by fitting empirical relaxation models to describe the relaxation towards two-phase equilibrium. For CO_2, these models have limited accuracy and a strong bias towards underprediction.

We argue that a missing component from relaxation models presented in the literature for CO_2 is the presence of a metastable single-phase fluid and a delay in the onset of the phase transition. In the literature, the most frequently used boiling delay models use the depressurization rate as a key variable. As the depressurization rate is not a state variable of the fluid, this complicates the calculations.

Two methods have been presented to investigate this in further detail: 1) the Delayed homogeneous relaxation model (Delayed HRM), and 2) the Metastable Isentrope Model (MIM). Delayed HRM is a new relaxation model that can readily be incorporated into a distributed description of the fluid flow, e.g. in CFD simulations or ejector models. MIM assumes isentropic flow, instantaneous equilibrium at the limit of metastability, and obtains the critical mass flow rate as the solution of a set of algebraic equations. The purpose of MIM is to estimate the critical mass flow rate by using the fluid description (the equation of state) and the limit of metastability as input.

When comparing the two methodologies to available experimental data on the critical mass flow rates of liquid CO_2 and H_2O through nozzles, we find that they give nearly the same predictions. This is because the critical mass flow rate is mostly determined by the onset of cavitation, and to a lesser extent by its relaxation towards equilibrium. A sensitivity study of the relaxation parameter used in Delayed HRM confirmed this.

At sufficiently high temperatures, homogeneous nucleation theory was found to represent the limit of metastability well. Using this limit as input, Delayed HRM and MIM deviated on average 11% from experimental data for CO_2 without the need for fitting parameters. In comparison, the best relaxation model available in the literature underpredicts the experimental data by 18% on average even after employing several fitting parameters. When homogeneous nucleation theory was used to represent the limit of metastability, the best agreement was found with experiments that employed PAG oil, which is hypothesized to suppress heterogeneous cavitation. This implies that flow rate measurements with and without such oil are qualitatively different. It also suggests the possibility that coating the nozzle with a smooth substrate to which the liquid is wetting can enhance the critical mass flow rate of liquids. Such methods can potentially be leveraged in engineering applications to improve the performance of ejectors.

It was found that the limit of metastability in nozzles at lower temperatures had to be predicted by heterogeneous nucleation theory. The experimental data displayed a crossover between homogeneous and heterogeneous nucleation at $T\approx285$ K for CO_2 and $T\approx590$ K for H_2O. For H_2O, we found that the predicted limit of metastability collapsed onto a single curve in the temperature–pressure space, where an expression was regressed for this curve. This suggests that the superheat limit is independent of the depressurization rate, at least for the experiments considered in the present work. By combining this expression with the above methodologies, we obtained an average deviation of 3% with available experimental data on H_2O.

The present work points at several topics for future work. One is to theoretically explain the high degree of collapse of superheat limits for different geometries, as deduced from critical mass flux data, and reconcile it with the exponential temperature dependence of the work reduction factor in heterogeneous nucleation theory. A second is to experimentally verify and refine the empirical correlation for the limit of superheat for H_2O, using more conventional measuring techniques for superheat limits, and to extend it to other fluids. A third possible topic is to generalize the findings in this work to other geometries such as orifices, pipe breaks, tubes, and slits, and to apply it to condensing flows.

Declaration of Competing Interest

The authors declare that they have no known competing financial interests or personal relationships that could have appeared to influence the work reported in this paper.

Acknowledgments

The authors acknowledge helpful discussions with Krzysztof Banasiak and Morten Hammer. This paper has been supported by the European Union's Horizon 2020 research and innovation programme under grant agreement NO 884213, project FRIENDSHIP. It has also received funding from the project Snow for the Future, financed by the Norwegian Ministry of Culture and the Ministry of Climate and Environment. The discussions in the paper reflect only the authors' views and the funding agents are not responsible for any use that may be made of the information that the paper contains.

Appendix A. Empirical heterogeneous nucleation limit for water

The empirical correlation fitted for the heterogeneous nucleation limit for water, $T_{\mathrm{shl}}(P)$, is a piecewise defined function of the pressure. For pressures below $P_{\mathrm{min}} = 1$ bar, the attainable superheat is so close to the saturation curve that

$$T_{\mathrm{shl}}(P) = T_{\mathrm{sat}}(P), \quad P < P_{\mathrm{min}}. \tag{A.1}$$

For pressures between P_{min} and $P_{\mathrm{max}} = 50$ bar, the correlation is

$$T_{\mathrm{shl}}(P) = a/y^2 + b/y + c + dy + ey^2, \quad P_{\mathrm{min}} \leqslant P \leqslant P_{\mathrm{max}}, \tag{A.2}$$

where $y = \ln P$, and P is in units of Pascal. The five coefficients are given in Table 3.

Table 3
Coefficients for the empirical correlation in Eq. (A.2).

a (K)	-1.845892×10^7
b (K)	5.512128×10^6
c (K)	-6.135645×10^5
d (K)	3.018692×10^4
e (K)	-5.516110×10^2

For higher pressures, as a first approximation one can use a simple linear extrapolation

$$T_{\mathrm{shl}}(P) = (1-\xi)T_{\mathrm{shl}}(P_{\mathrm{max}}) + \xi T_{\mathrm{crit}}, \quad P_{\mathrm{max}} < P \leqslant P_{\mathrm{crit}}, \tag{A.3}$$

where $\xi = (P - P_{\mathrm{max}})/(P_{\mathrm{crit}} - P_{\mathrm{max}})$. This correlation overpredicts the attainable superheat close to the critical point, and a more accurate correlation would be to use the homogeneous limit of superheat.

Appendix B. Sensitivity analyses

We have performed sensitivity analyses of key parameters used in this work. First, we will discuss the sensitivity of our results to the chosen value $J_{\mathrm{onset}} = 10^{13}$ m^{-3}s^{-1}. In Fig. 8 we show the effect of reducing J_{onset} by a factor of one million. Since the onset of cavitation will then happen at a lower degree of superheat, the predicted critical mass flow rates are lower. However, the effect is systematic and below the experimental uncertainty. The conclusions made in the present work are therefore insensitive to the exact value chosen for J_{onset}.

Next, we show that Delayed HRM and MIM give nearly identical predictions of the critical mass flow rates. Fig. 9 demonstrates that the assumption of isentropic flow before the cavitation occurs is an excellent approximation, seeing as the predictions on the left plot (isentropic models) yield very similar deviations from the mea-

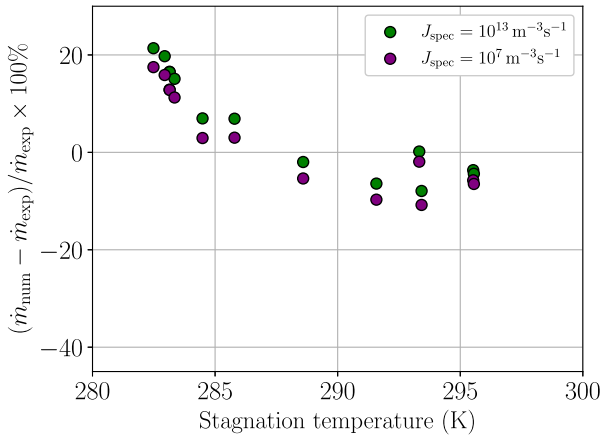

Fig. 8. The effect of the choice of onset cavitation rate J_{onset} for the CO_2 measurements by Haida et al. (2018).

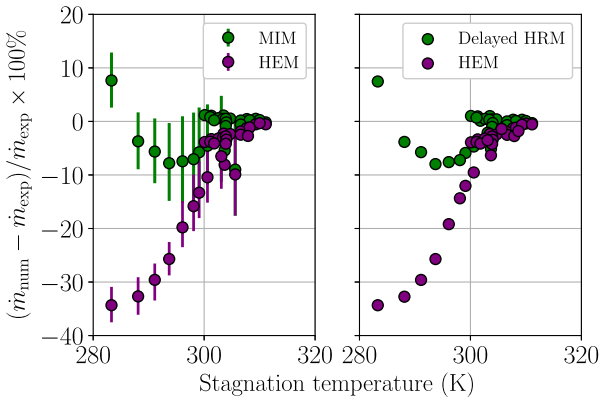

Fig. 9. Deviation in predictions from four different models of the critical mass flow rate against the CO_2 measurements of Haida et al. (2018). Left: Results for the MIM and isentropic HEM model with included uncertainties, same as Fig. 3 a). Right: Results for the full HRM model and the full (non-isentropic) HEM model.

surements as the predictions on the right plot (non-isentropic models.).

References

Aasen, A., Hammer, M., Skaugen, G., Jakobsen, J.P., Wilhelmsen, Ø., 2017. Thermodynamic models to accurately describe the PVTxy-behavior of water/carbon dioxide mixtures. Fluid Phase Equilib. 442, 125–139. https://doi.org/10.1016/j.fluid.2017.02.006.

Aasen, A., Blokhuis, E.M., Wilhelmsen, Ø., 2018. Tolman lengths and rigidity constants of multicomponent fluids: fundamental theory and numerical examples. J. Chem. Phys. 148 (20), 204702. https://doi.org/10.1063/1.5026747.

Aasen, A., Reguera, D., Wilhelmsen, Ø., 2020. Curvature corrections remove the inconsistencies of binary classical nucleation theory. Phys. Rev. Lett. 124, 045701. https://doi.org/10.1103/PhysRevLett.124.045701.

M. Alamgir, J. Lienhard, Correlation of pressure undershoot during hot-water depressurization, J. Heat Transfer (1981) doi:10.1115/1.3244429.

M. Alamgir, C. Kan, J. Lienhard, An experimental study of the rapid depressurization of hot water, J. Heat Transfer (1980). doi:10.1115/1.3244318.

C. Amos, V. Schrock, Critical discharge of initially subcooled water through slits, Tech. rep., Lawrence Berkeley Lab., CA (USA) (1983).

W. Angielczyk, Y. Bartosiewicz, D. Butrymowicz, J.-M. Seynhaeve, 1-D Modeling Of Supersonic Carbon Dioxide Two-Phase Flow Through Ejector Motive Nozzle, in: International Refrigerant and Air Conditioning Conference, 2010, pp. 1–8. URL http://docs.lib.purdue.edu/iracc/1102

Angielczyk, W., Seynhaeve, J.M., Gagan, J., Bartosiewicz, Y., Butrymowicz, D., 2019. Prediction of critical mass rate of flashing carbon dioxide flow in convergent-divergent nozzle. Chem. Eng. Process. Process. Intensif. 143, 107599. https://doi.org/10.1016/j.cep.2019.107599.

Attou, A., Seynhaeve, J.-M., 1999. Steady-state critical two-phase flashing flow with possible multiple choking phenomenon: Part 1: physical modelling and numerical procedure. J. Loss Prevent. Proc. 12 (5), 335–345.

Aursand, P., Gjennestad, M.Aa., Aursand, E., Hammer, M., Wilhelmsen, Ø., 2017. The spinodal of single-and multi-component fluids and its role in the development of modern equations of state. Fluid Phase Equilib. 436, 98–112. https://doi.org/10.1016/j.fluid.2016.12.018.

Avedisian, C.T., 1985. The homogeneous nucleation limits of liquids. J. Phys. Chem. Ref. Data 14 (3), 695–729. https://doi.org/10.1063/1.555734.

Awad, M.M., Muzychka, Y.S., 2008. Effective property models for homogeneous twophase flows. Exp. Therm. Fluid Sci. 33, 106–113.

Banasiak, K., Hafner, A., 2011. 1D Computational model of a two-phase R744 ejector for expansion work recovery. Int. J. Therm. Sci. 50, 2235–2247.

Banasiak, K., Hafner, A., 2013. Mathematical modelling of supersonic two-phase R744 flows through converging–diverging nozzles: The effects of phase transition models. Appl. Therm. Eng. 51 (1–2), 635–643.

Banasiak, K., Hafner, A., Kriezi, E.E., Madsen, K.B., Birkelund, M., Fredslund, K., Olsson, R., 2015. Development and performance mapping of a multi-ejector expansion work recovery pack for R744 vapour compression units. Int. J. Refrig. 57, 265–276. https://doi.org/10.1016/j.ijrefrig.2015.05.016.

Blander, M., Katz, J.L., 1975. Bubble nucleation in Liquids. AIChE J. 21 (5), 833–848. https://doi.org/10.1002/aic.690210502.

Boccardi, G., Bubbico, R., Celata, G.P., Mazzarotta, B., 2005. Two-phase flow through pressure safety valves. experimental investigation and model prediction. Chem. Eng. Sci. 60 (19), 5284–5293. https://doi.org/10.1016/j.ces.2005.04.032.

J. Bodys, J. Smolka, M. Palacz, M. Haida, K. Banasiak, Non-equilibrium approach for the simulation of CO_2 expansion in two-phase ejector driven by subcritical motive pressure, Int. J. Refrig. (2020) doi:10.1016/j.ijrefrig.2020.02.015.

Burnell, J., 1947. Flow of boiling water through nozzles, orifices and pipes. Engineering 164, 572–576.

Caupin, F., Herbert, E., 2006. Cavitation of Water: a Review. C.R. Phys. 7, 1000. https://doi.org/10.1016/j.crhy.2006.10.015.

Churchill, S.W., 1977. Friction factor equation spans all fluid flow regimes. Chem. Eng. 84, 91–92.

Dang, C., Hoshika, K., Hihara, E., 2012. Effect of lubricating oil on the flow and heat-transfer characteristics of supercritical carbon dioxide. Int. J. Refrig. 35 (5), 1410–1417. https://doi.org/10.1016/j.ijrefrig.2012.03.015.

Debenedetti, P., 1996. Metastable Liquids: Concepts and Principles. Princeton University Press, Princeton.

Deligiannis, P., Cleaver, J., 1992. Determination of the heterogeneous nucleation factor during a transient liquid expansion. Int. J. Multiphase Flow 18 (2), 273–278. https://doi.org/10.1016/0301-9322(92)90088-X.

Downar-Zapolski, P., Bilicki, Z., Bolle, L., Franco, J., 1996. The non-equilibrium relaxation model for one-dimensional flashing liquid flow. Int. J. Multiphase Flow 22 (3), 473–483. https://doi.org/10.1016/0301-9322(95)00078-X.

Eckhoff, R.K., 2014. Boiling liquid expanding vapour explosions (BLEVEs): A brief review. J. Loss Prevent. Proc. 32, 30–43. https://doi.org/10.1016/j.jlp.2014.06.008.

Fan, X., Wang, Y., Zhou, Y., Chen, J., Huang, Y., Wang, J., 2018. Experimental study of supercritical CO_2 leakage behavior from pressurized vessels. Energy 150, 342–350. https://doi.org/10.1016/j.energy.2018.02.147. http://www.sciencedirect.com/science/article/pii/S0360544218303815.

Friedrich, H., Vetter, G., 1962. Influence of nozzle shape on the through flow behavior of jets for water at various thermodynamic states. Energie 14, 3.

Giacomelli, F., Mazzelli, F., Banasiak, K., Hafner, A., Milazzo, A., 2019. Experimental and computational analysis of a R744 flashing ejector. Int. J. Refrig. 107, 326–343. https://doi.org/10.1016/j.ijrefrig.2019.08.007.

Haida, M., Smolka, J., Hafner, A., Palacz, M., Banasiak, K., Nowak, A.J., 2018. Modified homogeneous relaxation model for the R744 trans-critical flow in a two-phase ejector. Int. J. Refrig. 85, 314–333.

R. Hendricks, R. Simoneau, R. Ehlers, Choked flow of fluid nitrogen with emphasis on the thermodynamic critical region, Tech. Rep. TM X-68107, NASA, Cleveland, Ohio, USA (1972).

Hesson, J.C., Peck, R.E., 1958. Flow of two-phase carbon dioxide through orifices. AIChE J. 4 (2), 207–210. https://doi.org/10.1002/aic.690040216.

W. Ke, CO_2 BLEVE (boiling liquid expanding vapor explosion), Master's thesis, Høgskolen i Telemark (2009).

Kim, S.-M., Mudawar, I., 2015. Review of two-phase critical flow models and investigation of the relationship between choking, premature chf, and chf in micro-channel heat sinks. Int. J. Heat Mass Tran. 87, 497–511. https://doi.org/10.1016/j.ijheatmasstransfer.2015.04.012. URL http://www.sciencedirect.com/science/article/pii/S0017931015003725.

Levy, S., Abdollahian, D., 1982. Homogeneous non-equilibrium critical flow model. Int. J. Heat Mass Transf. 25 (6), 759–770.

Liao, Y., Lucas, D., 2017. Computational modelling of flash boiling flows: A literature survey. Int. J. Heat Mass Transf. 111, 246–265.

Lienhard, J.H., Karimi, A., 1981. Homogeneous nucleation and the spinodal line. J. Heat Transfer 103, 61–64. https://doi.org/10.1115/1.3244431.

Lienhard, J.H., Shamsundar, N., Biney, P.O., 1986. Spinodal lines and equations of state: A review. Nucl. Eng. Des. 95, 297–314. https://doi.org/10.1016/0029-5493(86)90056-7.

Moore, G.R., 1959. Vaporization of superheated drops in liquids. AIChE J. 5 (4), 458–466. https://doi.org/10.1002/aic.690050412.

Mulero, A., Cachadi na, I., Parra, M., 2012. Recommended correlations for the surface tension of common fluids. J. Phys. Chem. Ref. Data 41 (4), 043105. https://doi.org/10.1063/1.4768782.

Nakagawa, M., Berana, M.S., Kishine, A., 2009. Supersonic two-phase flow of CO_2 through converging–diverging nozzles for the ejector refrigeration cycle. Int. J. Refrig. 32 (6), 1195–1202. https://doi.org/10.1016/j.ijrefrig.2009.01.015.

Palacz, M., Haida, M., Smolka, J., Nowak, A.J., Banasiak, K., Hafner, A., 2017. HEM and HRM accuracy comparison for the simulation of CO_2 expansion in two-phase ejectors for supermarket refrigeration systems. Appl. Therm. Eng. 115, 160–169. https://doi.org/10.1016/j.applthermaleng.2016.12.122.

Pavlov, P.A., Skripov, V.P., 1970. Kinetics of spontaneous nucleation in strongly heated liquids. Teplofizika vysokikh temperatur 8 (3), 579–585.

T. Petrova, R.B. Dooley, Revised release on surface tension of ordinary water substance, Tech. rep., IAPWS (2014). URL http://www.iapws.org

Ringstad, K.E., Allouche, Y., Gullo, P., Ervik, Å., Banasiak, K., Hafner, A., 2020. A detailed review on CO_2 two-phase ejector flow modeling. Therm. Sci. Eng. Prog., 100647 https://doi.org/10.1016/j.tsep.2020.100647.

R.J. Simoneau, R.C. Hendricks, Two-phase choked flow of cryogenic fluids in converging-diverging nozzles, NASA Technical Paper 1484.

Span, R., Wagner, W., 1996. A New Equation of State for Carbon Dioxide Covering the Fluid Region from the Triple-Point Temperature to 1100 K at Pressures up to 800 MPa. J. Phys. Chem. Ref. Data 25, 1509.

Wagner, W., Pruß, A., 2002. The IAPWS Formulation 1995 for the Thermodynamic Properties of Ordinary Water Substance for General and Scientific Use. J. Phys. Chem. Ref. Data 31, 387. https://doi.org/10.1063/1.1461829.

Wahl, M.S., Aasen, A., Hjelme, D.R., Wilhelmsen, Ø., 2020. Ice formation and growth in supercooled water–alcohol mixtures: Theory and experiments with dual fiber sensors. Fluid Phase Equilib. 522, 112741. https://doi.org/10.1016/j.fluid.2020.112741.

Wakeshima, H., Takata, K., 1958. On the limit of superheat. J. Phys. Soc. Jpn. 13 (11), 1398–1403. https://doi.org/10.1143/JPSJ.13.1398.

Wilhelmsen, Ø., Skaugen, G., Hammer, M., Wahl, P.E., Morud, J.C., 2013. Time Efficient Solution of Phase Equilibria in Dynamic and Distributed Systems with Differential Algebraic Equation Solvers. Ind. Eng. Chem. Res. 52, 2130.

Wilhelmsen, Ø., Bedeaux, D., Kjelstrup, S., Reguera, D., 2014. Thermodynamic stability of nanosized multicomponent bubbles/droplets: The square gradient theory and the capillary approach. J. Chem. Phys. 140 (2), 024704. https://doi.org/10.1063/1.4860495.

Wilhelmsen, Ø., Aasen, A., Skaugen, G., Aursand, P., Austegard, A., Aursand, E., Gjennestad, M.A., Lund, H., Linga, G., Hammer, M., 2017. Thermodynamic Modeling with Equations of State: Present Challenges with Established Methods. Ind. Eng. Chem. Res. 56 (13), 3503–3515. https://doi.org/10.1021/acs.iecr.7b00317.

Xu, J., Chen, T., Chen, X., 1997. Critical flow in convergent-divergent nozzles with cavity nucleation model. Exp. Therm. Fluid Sci. 14 (2), 166–173. https://doi.org/10.1016/S0894-1777(96)00055-6.

Yin, S., Wang, H., Xu, B., Yang, C., Gu, H., 2020. Critical flow leakage of a vapour-liquid mixture from sub-cooled water: Nucleation boiling study. Int. J. Heat Mass Tran. 146, 118807. https://doi.org/10.1016/j.ijheatmasstransfer.2019.118807.

X. Zhou, K. Li, R. Tu, J. Yi, Q. Xie, X. Jiang, Numerical investigation of the leakage flow from a pressurized CO_2 pipeline, Energy Procedia 61 (2014) 151–154, international Conference on Applied Energy, ICAE2014. doi:10.1016/j.egypro.2014.11.927. http://www.sciencedirect.com/science/article/pii/S187661021402757X.

Zhu, X., Wang, D., Xu, C., Zhu, Y., Zhou, W., He, F., 2018. Structure influence on jet pump operating limits. Chem. Eng. Sci. 192, 143–160. https://doi.org/10.1016/j.ces.2018.05.054.